Molecular Pharmacology Fast Forward. Published on April 22, 2015 as DOI: 10.1124/mol.114.097485
This article has not been copyedited and formatted. The final version may differ from this version.

Anti-obesity effect of a small molecule repressor of RORγ

Mi Ra Chang, Yuanjun He, Tanya Khan, Dana S. Kuruvilla, Ruben Garcia-Ordonez, Cesar Corzo, Thaddeus J Unger, David W. White, Susan Khan, Li Lin, Michael D. Cameron, Theodore M. Kamenecka, and Patrick R. Griffin

Department of Molecular Therapeutics (M.R.C., Y.H., R.G-O, D.K., C.C., T.K., S.K., L.L, M.D.C., T.M.K., P.R.G)

The Scripps Research Institute, Jupiter, FL- 33458.USA

Ember Therapeutics (T.J.U, D.W.W.)

480 Arsenal Street, Watertown, MA- 02474,

Molecular Pharmacology Fast Forward. Published on April 22, 2015 as DOI: 10.1124/mol.114.097485
This article has not been copyedited and formatted. The final version may differ from this version.

Running Title: Pharmacological Inhibition of RORγ leads to decreased adiposity.

Corresponding Author: Patrick R. Griffin, The Scripps Research Institute, Scripps, Florida, 130 Scripps Way, Jupiter, FL 33458, pgriffin@scripps.edu

The number of text pages - 18

Number of Figures – 6

Number of supplement Figures - 7

Number of References - 37

Number of words in the:

Abstract - 182

Introduction – 612

Discussion – 531

Abbreviations: Diet induced obesity mice (DIO), RORγ (Retinoic acid receptor-related orphan receptor γ), Hormone sensing lipase (HSL), Uncoupling protein 1 (UCP1), Comprehensive lab animal monitoring system (CLAMS), Inguinal white adipose tissue (iWAT)

Molecular Pharmacology Fast Forward. Published on April 22, 2015 as DOI: 10.1124/mol.114.097485
This article has not been copyedited and formatted. The final version may differ from this version.

ABSTRACT

The orphan nuclear receptor RORγ is a key regulator for TH17 cell differentiation and it regulates metabolic and circadian rhythm genes in peripheral tissues. Previously it was shown that the small molecule inverse agonist of RORγ SR1555 suppressed TH17 differentiation and stimulated iTreg cells. Here we show that treatment of cultured pre-adipocyctes with SR1555 represses the expression of RORγ while leading to increased expression of FGF21 and adipoQ. Chronic administration of SR1555 to obese diabetic mice resulted in a modest reduction in food intake accompanied with significant reduction in fat mass resulting in reduced body weight and improved insulin sensitivity. Analysis *ex vivo* of treated mice demonstrates that SR1555 induced expression of the thermogenic gene program in fat depots. Further studies in cultured cells showed that SR1555 inhibited activation of hormone sensitive lipase and increased fatty acid oxidation. Combined, these results suggest that pharmacological repression of RORγ may represent a strategy for treatment of obesity by increasing thermogenesis and fatty acid oxidation, while inhibition of hormone sensitive lipase activity results in a reduction of serum free fatty acids leading to improved peripheral insulin sensitivity.

Molecular Pharmacology Fast Forward. Published on April 22, 2015 as DOI: 10.1124/mol.114.097485
This article has not been copyedited and formatted. The final version may differ from this version.

INTRODUCTION

The percentage of the global population categorized as overweight or obese has increased dramatically over the last few decades. This trend is predicted to continue as developed and developing nations increasingly adopt more sedentary lifestyles and gain easier access to high calorie diets. The metabolic syndrome is associated with obesity and patients with this syndrome are at a significant increased risk of suffering from cardiovascular disease and stroke (Moller & Kaufman, 2005). There are two major underlying drivers for the development of metabolic syndrome: excess adiposity (obesity) and Type 2 diabetes mellitus (T2DM) (Grundy et al, 2005). T2DM is a chronic metabolic disorder that results in part by the inability of the body to respond adequately to circulating insulin, a state of insulin resistance. In the obese state, free fatty acids (FFAs) are elevated in plasma and in all insulin responsive organs including skeletal muscle, liver and endothelial cells. As such, elevated FFAs are linked with the development of the metabolic syndrome. Obesity is also closely associated with a low grade state of inflammation characterized by elevated pro-inflammatory cytokines in blood and tissues (Tataranni & Ortega, 2005).

Treatments for metabolic syndrome included modification of diet and increased exercise (Grundy et al, 2004). However, pharmacologic intervention is typically required as weight loss and exercise often are not sufficient due to poor compliance and confounding genetic factors (Bouchard, 1988; Moller et al, 1996). Members of the nuclear receptor (NR) superfamily are ligand controlled

Molecular Pharmacology Fast Forward. Published on April 22, 2015 as DOI: 10.1124/mol.114.097485
This article has not been copyedited and formatted. The final version may differ from this version.

transcription factors that regulate a wide range of metabolic, endocrine and immunologic functions and this protein superfamily has proven to be a rich source of targets for the development of therapeutics for a wide range of human diseases including inflammation and diabetes. A subset of NRs are classified as orphan receptors due to lack of a characterized or agreed upon endogenous ligand (Kliewer et al, 1999). The retinoic acid receptor-related orphan receptor (ROR; NR1F) subfamily was identified based on sequence similarities to the retinoic acid and retinoid X receptors (Becker-Andre et al, 1993; Giguere et al, 1994). The T cell specific gamma isoform, RORγt, has been the focus of considerable attention due to its role in the development of T helper 17 cells (TH17) and in the pathology of autoimmune disease. While RORγt is highly expressed in immune cells and thymus, RORγ variants are expressed in the liver, skeletal muscle, adipose tissue, and kidney (Jetten, 2009), and its expression can be induced in macrophages during acute inflammatory responses (Barish et al, 2005; Chang et al, 2014; Gu et al, 2008). Furthermore, genetic deletion of RORγ results in profound effects on adipose depots with increased adipocyte number, yet reduced hypertrophy, accompanied by improved insulin sensitivity. These RORγ-deficient mice were shown to be resistant to diet-induced insulin resistance (Meissburger et al, 2011).

Recently, synthetic modulators of the ROR subfamily have been described (Kojetin & Burris, 2014; Marciano et al, 2014) including a series of reports on the development of potent and selective inverse agonists of RORγ. These studies demonstrate their utility in reducing the severity of inflammation in mouse models

Molecular Pharmacology Fast Forward. Published on April 22, 2015 as DOI: 10.1124/mol.114.097485
This article has not been copyedited and formatted. The final version may differ from this version.

of multiple sclerosis (experimental autoimmune encephalomyelitis, EAE) (Solt et al, 2011), and rheumatoid arthritis (collagen-induced arthritis, CIA) (Cascao et al, 2012; Chang et al, 2014; Huh et al, 2011). One such compound, SR1555, was previously shown to inhibit TH17 cell development while increasing the frequency of T regulatory (Treg) cells (Solt et al, 2012). Thus, SR1555 was evaluated in the CIA mouse model (Chang et al, 2014). In addition to observing a reduction in joint inflammation, effects on body weight and adiposity were noted. Based on this observation SR1555 was evaluated in the diet-induced obesity (DIO) murine model of obesity and T2DM and the results of these studies are presented in this report.

Molecular Pharmacology Fast Forward. Published on April 22, 2015 as DOI: 10.1124/mol.114.097485
This article has not been copyedited and formatted. The final version may differ from this version.

MATERIALS AND METHODS

Chemicals. SR1555 (**Fig. 1A**) was synthesized as previously described (Solt et al, 2012).

LanthaScreen TR-FRET Competitive Binding assay for PPARγ: The PPARγ competitive binding assay (Invitrogen) was performed according to the manufacturer's protocol. A mixture of 0.5 nM GST–PPARγ LBD, 5 nM Tb-GST-antibody, 5 nM fluormone Pan-PPAR Green, and serial dilutions of compound beginning at 10 µM downwards was added in 384-well low-volume plates (Greiner) to a total volume of 18 µl (2% DMSO in all wells). DMSO at 2% concentration was used as a no-ligand control. All dilutions were made in TR-FRET PPAR assay buffer. Experiments were performed in triplicate and incubated for 2 h in the dark before analysis in Perkin Elmer ViewLux ultra HTS microplate reader. TR-FRET signal was measured by excitation at 340 nm with emission at 520 nm for fluorescein and 490 nm for terbium. Data were plotted as the TR-FRET ratio 520/490nm using GraphPad Prism software.

Animals: Seventeen-week-old male C57BL/6 DIO mice were purchased from Jackson Laboratories. All procedures were approved and conducted in accordance to the Scripps Florida Institutional Animal Care and Use Committee. Mice were placed on a high-fat diet (HFD; 60% kcal derived from fat) for seven weeks until they reached an average weight of ~40g. Prior to and during compound administration mice were maintained on HFD. Animals were sham dosed with vehicle for three days prior to compound administration. SR1555 was administered intraperitoneally (i.p.) twice a day (BID) at 10 or 20mg/kg or per oral

Molecular Pharmacology Fast Forward. Published on April 22, 2015 as DOI: 10.1124/mol.114.097485
This article has not been copyedited and formatted. The final version may differ from this version.

(p.o.) at 20 mg/kg once-a-day (QD). Body weight and food intake were monitored daily. Pre- and post-experiment whole body composition analysis was performed on vehicle only and SR1555 treated mice using nuclear magnetic resonance (NMR, Minispec mq 7.5 NMR analyzer, Bruker Optics). Blood samples were collected for plasma cholesterol, triglyceride, free fatty acid and insulin measurements. For insulin tolerance tests, mice were injected (i.p.) with10mg/kg SR1555 for 18 days, and fasted 6 hrs before i.p. injection of Insulin (0.75 U/kg, Sigma aldrich). Blood glucose levels were measured at 0, 15, 30, 60, 90, 120 min using a glucometer (LifeScan). mice were allowed to recover from the stress associated with ITT for 7 days prior to performing the a glucose tolerance test (GTT). Here mice were fasted overnight before injection of 2 g/kg D- glucose i.p. and blood glucose levels were measured at 0, 15, 30, 60, 90, 120 min using a glucometer (LifeScan).

In vitro **adipocyte differentiation:** 3T3-L1 cells and C3H10T1/2 cells were maintained in Dulbecco's modified Eagle's medium (DMEM) supplemented with 10% FBS (Gibco BRL). Twenty-four hours post-confluence, the 3T3-L1 cells were differentiated with IBMX (0.5mM), dexamethasone (1μM), insulin (10 μg/ml) and 10% FBS for forty-eight hours. After induction of adipogenesis, the cells were maintained with insulin (10 μg/ml) and 20μM of SR1555 for three or four days. The stromal vascular fraction (SVF) within adipose tissue was isolated from the epididymal adipose tissue of C57BL/6 mice to avoid contamination from non-adipose tissues as previously described (Koh et al, 2007). To exclude blood contamination in the adipose tissue, systemic perfusion with heparinized PBS

Molecular Pharmacology Fast Forward. Published on April 22, 2015 as DOI: 10.1124/mol.114.097485
This article has not been copyedited and formatted. The final version may differ from this version.

was performed before harvesting or washing isolated adipose tissues with PBS. Then, the adipose tissues were incubated in Hanks balanced salt solution (HBSS; Sigma-Aldrich) containing 0.2% collagenase type 2 for 60 minutes at 37°C with constant shaking. After inactivation collagenase activity with 10% fetal bovine serum (FBS) containing Dulbecco modified eagle medium (DMEM), the cell suspension was filtered through a 40μm nylon mesh (BD Biosciences) followed by centrifugation at 420g for 5 minutes. Floating adipocytes and supernatant were removed from the SVF pellet. The SVF pellet was washed and re-suspended in sterilized PBS.

Quantitative real-time PCR: Total RNA was extracted from 3T3-L1 cells or tissues using TRIzol reagent (Invitrogen). The RNA was reverse-transcribed using the ABI reverse transcription kit. Quantitative PCR reactions were performed with SYBR green fluorescent dye using an ABI9300 PCR machine. Relative mRNA expression was determined by the ΔΔ-Ct method normalized to GAPDH levels. The sequences of primers used in this study are found in **Supplemental Fig. 1.**

Mitotracker-FACS quantification: C2C12 cells were washed with PBS, trypsinized and incubated at 37^{o}C for 20 min with 100 nM MiroTracker Green FM and Red GM dyes (Molecular Probes). Mitotracker Green probe preferentially accumulates in mitochondria, allowing estimation of mitochondrial quantity. Mitotracker Red probe is a red-fluorescent dye that stains mitochondria in living cells and its accumulation is dependent on the membrane potential (Molecular Probes). Samples were washed 3 times in PBS and subjected to flow cytometric

Molecular Pharmacology Fast Forward. Published on April 22, 2015 as DOI: 10.1124/mol.114.097485
This article has not been copyedited and formatted. The final version may differ from this version.

analysis on a BD LSRII instrument (Becton Dickinson, San Jose, CA), and the results were analyzed using FlowJo software (Tree Star).

Oxygen Consumption: Immortalized SVF cells were seeded at 1 x 10^4 cells per well in a differentiation medium containing DMEM with 10% FBS on XF-96 well culture plates (Seahorse). Cellular oxygen consumption rate was measured using the Seahorse XF96 at four to five days differentiation with 20μM SR1555. The concentration of fatty acid (oleic acid, Linoleic acid), oligomycin, FCC, rotenone were 1mg/mL, 10mg/mL, 6mM, 3mM, respectively.

Resting whole-body metabolic parameters: Daily average whole–body VO_2 (ml/kg/h), and cage activity (movement counts) were measured in DIO mice using a comprehensive laboratory animal monitoring system (CLAMS: Oxymax series; Columbus Instruments, Columbus, OH, USA). Each sealed chamber (CLAMS unit) is equipped with an O2 electrochemical sensor, a CO2 infrared sensor, and infrared beam activity sensors. The units allow the volume of O2 consumed (VO2; ml/kg/h) to be measured. Infrared beam interruptions in both horizontal (X) and vertical (Z) directions were measured to quantify the motor activity of mice in both directions. Total horizontal beam breaks are summed to provide total horizontal activity count or XTOT. Two or more consecutive horizontal beam breaks were recorded as ambulatory activity count (XAMB). All vertical beam breaks were summed to provide total vertical activity count or ZTOT. CLAMS studies began after animals were acclimated to the metabolic chambers, and VO_2 data were collected 16-min intervals over a 5 day period

Molecular Pharmacology Fast Forward. Published on April 22, 2015 as DOI: 10.1124/mol.114.097485
This article has not been copyedited and formatted. The final version may differ from this version.

under a consistent environmental temperature (22^{o}C). During these studies, mice were allowed free access to food and water.

Western blot analysis: Primary antibodies against phosphor-HSL (S660), total HSL and beta-actin were purchased from Cell Signaling Technology (CST). A rabbit fast western blotting kit (Pierce, Thermo scientific) was used for detection of primary antibody signal.

Plasma concentration of *FGF21* and Insulin: Blood samples were collected in heparin tubes on ice and centrifuged at 4°C. Endogenous FGF21 and Insulin levels were determined by a specific mouse enzyme-linked immunosorbent assay (ELISA) (Millipore, Billerica, MA) following manufacturer's instructions.

Plasma Lipid Profile: Blood samples were collected in heparin tubes on ice and centrifuged at 4°C. Cholesterol, triglyceride (TAG) and free fatty acid (FFA) were quantitated using a Cobas c311 clinical chemistry analyzer (Roche Diagnostics).

Pharmacokinetics: The oral pharmacokinetic profile of SR1555 was determined in male C57Bl6 mice. SR1555 was formulated at a concentration of 1 mg/ml in 15% cremophore EL in water and dosed by oral gavage to three mice at a final dose of 20 mg/kg. Blood was collected in lithium-heparin coated capillary tubes using a microsampling technique at 15, 30, 60, 120, 240, 360, 480, and 1440 minutes and plasma was generated using standard centrifugation methods. Plasma concentrations were determined via LC-MS/MS on an ABSciex 5500. SR1555 was detected using the mass transition 461→333, and concentrations were determined by comparison to a nine point standard curve between 2 and

Molecular Pharmacology Fast Forward. Published on April 22, 2015 as DOI: 10.1124/mol.114.097485
This article has not been copyedited and formatted. The final version may differ from this version.

2000 ng/ml prepared in mouse plasma. Pharmacokinetic analysis was done with WinNonLin, Pharsight inc. using a noncompartimental model. All procedures described are covered under existing protocols and have been approved by the Scripps Florida IACUC to be conducted in the Scripps vivarium, which is fully AAALAC accredited.

Statistical analysis: The data are reported as the mean ± SEM. Statistical significance was evaluated using Student's unpaired *t*-test. *P* values less than 0.05 were considered significant.

Molecular Pharmacology Fast Forward. Published on April 22, 2015 as DOI: 10.1124/mol.114.097485
This article has not been copyedited and formatted. The final version may differ from this version.

RESULTS

SR1555 alters adipogenesis. Previously, SR1555 (**Fig. 1A**) was shown to be a RORγ-specific inverse agonist that inhibited T_H17 cell development and increased the Treg cell population (Solt et al, 2012). Since genetic deletion of RORγ results in profound effects on adipose tissue we investigated the effects of SR1555 on adipogenesis using differentiated 3T3L1 cells. Treatment of these cells with SR1555 resulted in decreased expression of RORγ (**Fig. 1B**). Consistent with observations from RORγ-depleted mice, SR1555 treatment led to increased expression of *FABP4* (fatty acid binding protein; aP2) and *Adiponectin* (AdipoQ) but it had no effect on the expression of PPARγ, a key adipogenic regulator. Interestingly, the expression of *FGF21* (fibroblast growth factor 21) was increased in SR1555 treated 3T3L1 adipocytes. *FABP4* is a PPARG (*NR1C3*) target gene so we tested the ability of SR1555 to bind to this nuclear receptor. Consistent with results from broad selectivity profiling and as shown in **Supplemental Fig. 2A**, in a TR-FRET competitive binding assay, SR1555 was not able to displace labeled ligand at all concentrations tested. Furthermore, SR1555 was not able to transactivate the expression of luciferase in a reporter gene assay at all concentrations tested (**Supplemental Fig. 2B**).

RORγ-deficient mice are resistant to obesity and insulin resistance (Meissburger et al, 2011). Based on these observations, we sought to determine the effects of pharmacological repression of RORγ in the diet induced obesity (DIO) mouse model of obesity and diabetes. Mice were fed a HFD until reaching obesity (avg. weight of ~40g). DIO mice were then treated with vehicle (15%

Molecular Pharmacology Fast Forward. Published on April 22, 2015 as DOI: 10.1124/mol.114.097485
This article has not been copyedited and formatted. The final version may differ from this version.

cremophor, i.p.) for three days prior to initiating administration of SR1555. As shown in **Supplemental Fig. 3**, bolus administration of SR1555 to mice at 5mg/kg, 10mg/kg i.p., and 20mg/kg by oral gavage afforded plasma concentration of compound four hours post administration in excess of 4, 8, and 16μM, respectively. The calculated PK parameters are presented in **Supplemental Fig. 4**. With the intent of only partially repressing RORγ and based on the plasma exposure from the PK studies shown in **Supplemental Fig. 3**, SR1555 was administered i.p. to obese mice at 5mg/kg or 10mg/kg twice a day (BID). Body weight and food intake were recorded daily. Following 20 days of compound administration, DIO mice receiving vehicle only maintained body weight but animals treated with SR1555 at 5mg/kg had lost 15% of their body weight (**Fig. 2A**). SR1555 demonstrated a dose-dependent impact on body weight as mice administered compound at 10mg/kg lost an additional 8% body weight (23% loss). Compound treatment did cause a modest reduction in food intake by DIO mice as compared to control animals (**Fig. 2B**). However, no change in food intake was observed in lean mice suggesting SR1555 is not driving weight loss by systemic toxicity. It is possible that SR1555 treatment results in an improvement in leptin sensitivity.

Whole body composition of DIO mice was analyzed using NMR prior to the start of vehicle or compound administration and again at the conclusion of the study. As shown in **Fig. 2C**, lean mass was unaffected by SR1555 treatment; however, there was a statistically significant loss of fat mass in the 10mg/kg SR1555 treated DIO mice. On Day 18 of treatment, mice were fasted for 8 hours

Molecular Pharmacology Fast Forward. Published on April 22, 2015 as DOI: 10.1124/mol.114.097485
This article has not been copyedited and formatted. The final version may differ from this version.

and then subjected to an insulin tolerance test (ITT). As shown in **Fig. 3A** fasting insulin was significantly reduced in both the 5 and 10 mg/kg arms of the study. **Fig. 3B** illustrates that glucose disposal was improved with a quick decline in plasma glucose 15 min post insulin administration in the 10mg/kg arm of the study. Statistically significant differences in plasma glucose were observed at 30, 60 and 90 min post insulin administration. Following the ITT, compound administration was terminated and mice were allowed to recover from the stress of fasting. At seven days post compound administration a glucose tolerance test (GTT) was performed to determine if SR1555 treatment results in improved disposal of plasma glucose in response to a bolus intake of a glucose solution. As shown in **Fig. 3C**, DIO mice treated with SR1555 retained improved insulin sensitivity seven days post compound treatment. Analysis of plasma lipids at this time point showed that SR1555 treatment reduced cholesterol and triglyceride levels below vehicle only treated mice and to a level similar to that in control lean mice maintained on a normal chow diet (**Fig. 3D**). Free fatty acid levels were also reduced in SR1555 treated animals (**Fig. 3D**). Although SR1555 increased expression of FGF21 in adipocytes, compound treatment in DIO mice did not result in an increase in plasma FGF21 (data not shown) released from the liver.

We next investigated whether whole-body energy expenditure and ambulatory activity were impacted by SR1555 treatment. DIO mice were acclimated to single animal housing for seven days prior to the start of this study. SR1555 was then administered p.o. at 20mg/kg for 7 days before placing the animals in Comprehensive Lab Animal Monitoring System (CLAMS) chambers.

Molecular Pharmacology Fast Forward. Published on April 22, 2015 as DOI: 10.1124/mol.114.097485
This article has not been copyedited and formatted. The final version may differ from this version.

Once inside the CLAMS chambers, mice were administered SR1555 orally each day at 20 mg/kg and metabolic parameters and activity were evaluated over a seven-day period.

As shown in **Fig. 4A,** oxygen consumption (VO2) in compound treated DIO mice was increased during both the light and dark cycles as compared to the vehicle only treated group. Furthermore, body temperature was significantly increased in SR1555 treated mice (**Supplemental Fig. 5A and B**). No difference in XTOT and XAMB was observed when comparing SR1555 treated mice to vehicle only treated mice; however, ZTOT was increased in compound treated DIO mice (**Fig. 4B, C, D**). It is possible that this increase in vertical activity may reflect increased exploration of the environment (attention), cognitive enhancement, or perhaps anxiety. Regardless, the data obtained using CLAMS suggests that SR1555 stimulated activity and increased energy expenditure in DIO mice.

Induction of thermogenesis by SR1555. Uncoupling protein 1 (UCP1) is critical for heat generation and the protein is selectively expressed in brown and beige adipose cells. Classical brown adipose tissue (BAT) and inducible white adipocytes (beige cells) are capable of increasing energy expenditure through the uncoupling of oxidative metabolism from ATP (Wu et al, 2012; Wu et al, 2013). Also, previous physiological studies have shown that diet can induce thermogenesis in order to maintain body weight (Rothwell & Stock, 1997). Therefore, we asked whether SR1555 induces thermogenic genes in adipose depots in DIO mice. Inguinal white adipose tissue (iWAT) and brown adipose

Molecular Pharmacology Fast Forward. Published on April 22, 2015 as DOI: 10.1124/mol.114.097485
This article has not been copyedited and formatted. The final version may differ from this version.

tissue (BAT) were collected from DIO mice. Induction of UCP1 protein in iWAT and overall adipose size were smaller in SR1555 treated iWAT (**Fig. 5A**). Additionally, gene expression of UCP1, PRDM16 and FGF21 were increased in BAT from SR1555 treated mice as compared to tissue from vehicle only treated mice. The expression of 18S gene was used as a control to determine relative expression of thermogenic genes (**Fig. 5B**).

FABP4 (aP2) gene expression was also increased by SR1555 treatment and this phenotype was similar to that observed with genetic depletion of RORγ (Meissburger et al, 2011). Induction of UCP1 gene expression was also observed in the brown cell adipogenic process using C3H10T1-2 cells (**Fig. 5C**) where the effect of SR1555 treatment was similar to that of TZD treatment which was the positive control for the assay (Ohno et al, 2012). Furthermore, SR1555 increased the mitochondrial membrane potential and mass in C2C12 cells (**Fig. 6A**). Taken together, we conclude that SR1555 induces the thermogenic gene program and alters mitochondrial potential in adipose and muscle cell lines.

Fatty Acid Oxidation and Lipolysis. The reduction of FFAs observed in obese mice treated with SR1555 could be the result of increased FFA storage, increase degradation of FFAs by β-oxidation, decrease in lipolysis of triglycerides, or a combination of these events. The effect of SR1555 on fatty acid oxidation was monitored in immortalized stromal vascular fraction (SVF) cells. Differentiation is achieved *in vitro* by sequential application of adipogenic factors to pre-adipocytes over a period of several days. Following differentiation, adipocytes were characterized using the XF Analyzer from Seahorse Bioscience to measure four

Molecular Pharmacology Fast Forward. Published on April 22, 2015 as DOI: 10.1124/mol.114.097485
This article has not been copyedited and formatted. The final version may differ from this version.

essential parameters of mitochondrial function: basal respiration, ATP turnover, proton leak, and maximal respiration. Fatty acid oxidation in mitochondria is mainly controlled by CPT-1, which facilitates transport of long chain fatty acids into mitochondria. CPT-1 was unchanged in SR1555 treated SVF cells. However, oxygen consumption was increased at four independent time points following addition of fatty acid mixture (oleic acid and linoleic acid) whereas no increase was observed in DMSO only treated SVF cells (**Fig. 6B**). Next, we evaluated the activity of hormone sensitive lipase (HSL) in differentiated 3T3L1 cells following SR1555 treatment (**Supplemental Fig. 6**). Elevated plasma levels of free fatty acids (FFAs) are thought to play a major role in the pathogenesis of insulin resistance and type 2 diabetes by inhibiting glucose uptake and utilization by muscle and causing increased glucose output by the liver (Claus et al, 2005; Girousse et al, 2013). Here we observed that HSL gene expression and phosphorylated HSL (S660) were reduced in fully differentiated 3T3L1 cells. Therefore, we suggest that decreasing phosphorylated HSL might drive the reduction of FFA release from white adipocytes.

Molecular Pharmacology Fast Forward. Published on April 22, 2015 as DOI: 10.1124/mol.114.097485
This article has not been copyedited and formatted. The final version may differ from this version.

DISCUSSION

The nuclear receptor superfamily of ligand regulated transcription factors has proven to be a rich source of targets for the development of therapeutics for a wide range of human diseases. Within the NR1F subfamily of NRs, RORyt has garnered much attention due to its role in Th17 cells. However, its contribution to obesity and insulin resistance has been recently demonstrated (Meissburger et al, 2011; Takeda et al, 2014). The discovery that the potent LXR agonist T0901317 also functioned as an inverse agonist for RORα and RORγ (Kumar et al, 2010) led to an explosion in medicinal chemistry efforts focused on the NR1F subfamily of receptors. This effort is exemplified by publications of the RORα/γ agonist SR1078 (Wang et al, 2010), the selective RORα inverse agonist SR3335 (Kumar et al, 2011), the dual RORα/γ inverse agonist SR1001 (Solt et al, 2011), and the selective RORγ inverse agonist SR2211 (Kumar et al, 2012) and SR1555 (Solt et al, 2012). Here we demonstrate that the selective RORγ inverse agonist SR1555 recapitulates many of RORG depletion phenotype in terms of adiposity and metabolic parameters. Specifically, SR1555 treatment of obese and diabetic mice modulated adipocyte function leading to body weight loss exclusively as a result of reduced adiposity leading to improved insulin sensitivity and glucose disposal.

It is possible that SR1555-mediated improvement in metabolic phenotype involves the modulation of Treg development. Previously it was shown that in cultured cells SR1555 repressed Th17 cell differentiation with concomitant

Molecular Pharmacology Fast Forward. Published on April 22, 2015 as DOI: 10.1124/mol.114.097485
This article has not been copyedited and formatted. The final version may differ from this version.

expansion of inducible Tregs (Solt et al, 2012), and induction of Tregs have been shown to be associated with metabolic disorders (Bhat et al, 2014; Michalek et al, 2011). Additionally, obese individuals with insulin resistance display a sharp reduction of Treg's (DeFuria et al, 2013), and depletion of Treg's in mice using an anti-CD25 monoclonal antibody exacerbates insulin resistance (Eller et al, 2011). Previously, we had shown that SR1555 was capable of suppressing inflammatory cytokine production such as IL-6 and TNF-α in LPS-stimulated RAW264.7 cells (Chang et al, 2014). Therefore, it is possible that the anti-inflammatory actions of SR1555 are associated with its ability to improve adiposity and metabolic parameters.

Treatment of 3T3L1 cells with SR1555 resulted in inhibition of the enzyme hormone-sensitive lipase (HSL; EC 3.1.1.79). HSL is highly expressed in adipose tissue and is a major contributor to the formation FFAs in fat. Release of these FFAs provides a source of energy for most tissues. HSL activity is the rate-limiting step in catecholamine-induced lipolysis and the level of HSL expression is directly related to the lipolytic capacity of mature fat cells (Large et al, 1998). These initial findings suggested that increased HSL activity may contribute to the increased plasma FFAs observed in obesity. Interestingly, partial inhibition of lipolysis in adipose tissue in HSL haplo-insufficient mice ($HSL^{+/-}$) resulted in improved insulin sensitivity (Girousse et al, 2013). Analysis of the promoter region of HSL (LIPE) suggests it contains four putative RORE sequences (**Supplemental Fig 7. A and B**). Thus, it is plausible that HSL expression and activity are regulated by RORγ. Previous CHiP-Seq data demonstrated that

Molecular Pharmacology Fast Forward. Published on April 22, 2015 as DOI: 10.1124/mol.114.097485
This article has not been copyedited and formatted. The final version may differ from this version.

RORg binds to the promoter of family members of HSL. It remains to be determined if SR1555 mediated repression of HSL activity is direct or indirect.

Furthermore, SR1555 treatment increased gene expression and protein levels of UCP1, altered mitochondrial potential, and increased the level of fatty acid oxidation in both brown adipocytes and beige cells suggesting that RORγ regulates the oxidative phosphorylation process in mitochondria. In summary, the selective RORγ inverse agonist SR1555 may provide a useful starting point for the development of peripheral acting therapeutics for the treatment of diabetes and obesity.

ACKNOWLEDGMENTS

The authors thank Melissa Kazantzis for assistance with metabolic studies and Mohammad Fallahi-Sichani for bioinformatic support.

Molecular Pharmacology Fast Forward. Published on April 22, 2015 as DOI: 10.1124/mol.114.097485
This article has not been copyedited and formatted. The final version may differ from this version.

AUTHORSHIP CONTRIBUTIONS:

Participated in research design: Chang, Kamenecka, White, Griffin, Cameron

Conducted experiments: Chang, Garcia-Ordonez, Kuruvilla, T. Khan, S. Khan, Lin, Unger

Contributed new reagents or analytic tools: He, Kamenecka

Performed data analysis: Chang, Unger, White, Griffin, Cameron

Wrote or contributed to the writing of the manuscript: Chang, Corzo, Griffin, Cameron

Molecular Pharmacology Fast Forward. Published on April 22, 2015 as DOI: 10.1124/mol.114.097485
This article has not been copyedited and formatted. The final version may differ from this version.

References

Barish GD, Downes M, Alaynick WA, Yu RT, Ocampo CB, Bookout AL, Mangelsdorf DJ, Evans RM (2005) A Nuclear Receptor Atlas: macrophage activation. *Mol Endocrinol* **19:** 2466-2477

Becker-Andre M, Andre E, DeLamarter JF (1993) Identification of nuclear receptor mRNAs by RT-PCR amplification of conserved zinc-finger motif sequences. *Biochem Biophys Res Commun* **194:** 1371-1379

Bhat PK, K NH, Idris M, Christopher P, Rai N (2014) Modified distal shoe appliance for premature loss of multiple deciduous molars: a case report. *Journal of clinical and diagnostic research : JCDR* **8:** ZD43-45

Bouchard C (1988) Genetic factors in the regulation of adipose tissue distribution. *Acta Med Scand Suppl* **723:** 135-141

Cascao R, Vidal B, Raquel H, Neves-Costa A, Figueiredo N, Gupta V, Fonseca JE, Moita LF (2012) Effective treatment of rat adjuvant-induced arthritis by celastrol. *Autoimmun Rev* **11:** 856-862

Chang MR, Lyda B, Kamenecka TM, Griffin PR (2014) Pharmacologic repression of retinoic acid receptor-related orphan nuclear receptor gamma is therapeutic in the collagen-induced arthritis experimental model. *Arthritis Rheumatol* **66:** 579-588

Claus TH, Lowe DB, Liang Y, Salhanick AI, Lubeski CK, Yang L, Lemoine L, Zhu J, Clairmont KB (2005) Specific inhibition of hormone-sensitive lipase improves lipid profile while reducing plasma glucose. *J Pharmacol Exp Ther* **315:** 1396-1402

DeFuria J, Belkina AC, Jagannathan-Bogdan M, Snyder-Cappione J, Carr JD, Nersesova YR, Markham D, Strissel KJ, Watkins AA, Zhu M, Allen J, Bouchard J, Toraldo G, Jasuja R, Obin MS, McDonnell ME, Apovian C, Denis GV, Nikolajczyk BS (2013) B cells promote inflammation in obesity and type 2 diabetes through regulation of T-cell function and an inflammatory cytokine profile. *Proceedings of the National Academy of Sciences of the United States of America* **110:** 5133-5138

Eller K, Kirsch A, Wolf AM, Sopper S, Tagwerker A, Stanzl U, Wolf D, Patsch W, Rosenkranz AR, Eller P (2011) Potential role of regulatory T cells in reversing obesity-linked insulin resistance and diabetic nephropathy. *Diabetes* **60:** 2954-2962

Giguere V, Tini M, Flock G, Ong E, Evans RM, Otulakowski G (1994) Isoform-specific amino-terminal domains dictate DNA-binding properties of ROR alpha, a novel family of orphan hormone nuclear receptors. *Genes & development* **8:** 538-553

Girousse A, Tavernier G, Valle C, Moro C, Mejhert N, Dinel AL, Houssier M, Roussel B, Besse-Patin A, Combes M, Mir L, Monbrun L, Bezaire V, Prunet-Marcassus B, Waget A, Vila I, Caspar-Bauguil S, Louche K, Marques MA, Mairal A, Renoud ML, Galitzky J, Holm C, Mouisel E, Thalamas C, Viguerie N, Sulpice T, Burcelin R, Arner P, Langin D (2013) Partial inhibition of adipose tissue lipolysis improves glucose metabolism and insulin sensitivity without alteration of fat mass. *PLoS Biol* **11:** e1001485

Grundy SM, Cleeman JI, Daniels SR, Donato KA, Eckel RH, Franklin BA, Gordon DJ, Krauss RM, Savage PJ, Smith SC, Jr., Spertus JA, Costa F (2005) Diagnosis and management of the metabolic syndrome: an American Heart Association/National Heart, Lung, and Blood Institute Scientific Statement. *Circulation* **112:** 2735-2752

Grundy SM, Hansen B, Smith SC, Jr., Cleeman JI, Kahn RA (2004) Clinical management of metabolic syndrome: report of the American Heart Association/National Heart, Lung, and Blood Institute/American Diabetes Association conference on scientific issues related to management. *Circulation* **109:** 551-556

Gu Y, Yang J, Ouyang X, Liu W, Li H, Yang J, Bromberg J, Chen SH, Mayer L, Unkeless JC, Xiong H (2008) Interleukin 10 suppresses Th17 cytokines secreted by macrophages and T cells. *Eur J Immunol* **38:** 1807-1813

Huh JR, Leung MW, Huang P, Ryan DA, Krout MR, Malapaka RR, Chow J, Manel N, Ciofani M, Kim SV, Cuesta A, Santori FR, Lafaille JJ, Xu HE, Gin DY, Rastinejad F, Littman DR (2011) Digoxin and its derivatives suppress TH17 cell differentiation by antagonizing RORgammat activity. *Nature* **472:** 486-490

Jetten AM (2009) Retinoid-related orphan receptors (RORs): critical roles in development, immunity, circadian rhythm, and cellular metabolism. *Nucl Recept Signal* **7:** e003

Kliewer SA, Lehmann JM, Willson TM (1999) Orphan nuclear receptors: shifting endocrinology into reverse. *Science* **284:** 757-760

Koh YJ, Kang S, Lee HJ, Choi TS, Lee HS, Cho CH, Koh GY (2007) Bone marrow-derived circulating progenitor cells fail to transdifferentiate into adipocytes in adult adipose tissues in mice. *J Clin Invest* **117:** 3684-3695

Kojetin DJ, Burris TP (2014) REV-ERB and ROR nuclear receptors as drug targets. *Nat Rev Drug Discov* **13:** 197-216

Kumar N, Kojetin DJ, Solt LA, Kumar KG, Nuhant P, Duckett DR, Cameron MD, Butler AA, Roush WR, Griffin PR, Burris TP (2011) Identification of SR3335 (ML-176): a synthetic RORalpha selective inverse agonist. *ACS chemical biology* **6:** 218-222

Kumar N, Lyda B, Chang MR, Lauer JL, Solt LA, Burris TP, Kamenecka TM, Griffin PR (2012) Identification of SR2211: a potent synthetic RORgamma-selective modulator. *ACS chemical biology* **7:** 672-677

Kumar N, Solt LA, Conkright JJ, Wang Y, Istrate MA, Busby SA, Garcia-Ordonez RD, Burris TP, Griffin PR (2010) The benzenesulfoamide T0901317 [N-(2,2,2-trifluoroethyl)-N-[4-[2,2,2-trifluoro-1-hydroxy-1-(trifluoromethyl)ethy l]phenyl]-benzenesulfonamide] is a novel retinoic acid receptor-related orphan receptor-alpha/gamma inverse agonist. *Molecular pharmacology* **77:** 228-236

Large V, Arner P, Reynisdottir S, Grober J, Van Harmelen V, Holm C, Langin D (1998) Hormone-sensitive lipase expression and activity in relation to lipolysis in human fat cells. *J Lipid Res* **39:** 1688-1695

Marciano DP, Chang MR, Corzo CA, Goswami D, Lam VQ, Pascal BD, Griffin PR (2014) The therapeutic potential of nuclear receptor modulators for treatment of metabolic disorders: PPARgamma, RORs, and Rev-erbs. *Cell Metab* **19:** 193-208

Meissburger B, Ukropec J, Roeder E, Beaton N, Geiger M, Teupser D, Civan B, Langhans W, Nawroth PP, Gasperikova D, Rudofsky G, Wolfrum C (2011) Adipogenesis and insulin sensitivity in obesity are regulated by retinoid-related orphan receptor gamma. *EMBO Mol Med* **3:** 637-651

Michalek RD, Gerriets VA, Jacobs SR, Macintyre AN, MacIver NJ, Mason EF, Sullivan SA, Nichols AG, Rathmell JC (2011) Cutting edge: distinct glycolytic and lipid oxidative metabolic programs are essential for effector and regulatory CD4+ T cell subsets. *J Immunol* **186:** 3299-3303

Moller DE, Bjorbaek C, Vidal-Puig A (1996) Candidate genes for insulin resistance. *Diabetes Care* **19:** 396-400

Moller DE, Kaufman KD (2005) Metabolic syndrome: a clinical and molecular perspective. *Annu Rev Med* **56:** 45-62

Ohno H, Shinoda K, Spiegelman BM, Kajimura S (2012) PPARgamma agonists induce a white-to-brown fat conversion through stabilization of PRDM16 protein. *Cell metabolism* **15:** 395-404

Rothwell NJ, Stock MJ (1997) A role for brown adipose tissue in diet-induced thermogenesis. *Obes Res* **5:** 650-656

Solt LA, Kumar N, He Y, Kamenecka TM, Griffin PR, Burris TP (2012) Identification of a selective RORgamma ligand that suppresses T(H)17 cells and stimulates T regulatory cells. *ACS chemical biology* **7:** 1515-1519

Solt LA, Kumar N, Nuhant P, Wang YJ, Lauer JL, Liu J, Istrate MA, Kamenecka TM, Roush WR, Vidovic D, Schurer SC, Xu JH, Wagoner G, Drew PD, Griffin PR, Burris TP (2011) Suppression of T(H)17 differentiation and autoimmunity by a synthetic ROR ligand. *Nature* **472:** 491-494

Takeda Y, Kang HS, Freudenberg J, DeGraff LM, Jothi R, Jetten AM (2014) Retinoic acid-related orphan receptor gamma (RORgamma): a novel participant in the diurnal regulation of hepatic gluconeogenesis and insulin sensitivity. *PLoS genetics* **10:** e1004331

Tataranni PA, Ortega E (2005) A burning question: does an adipokine-induced activation of the immune system mediate the effect of overnutrition on type 2 diabetes? *Diabetes* **54:** 917-927

Wang Y, Kumar N, Nuhant P, Cameron MD, Istrate MA, Roush WR, Griffin PR, Burris TP (2010) Identification of SR1078, a synthetic agonist for the orphan nuclear receptors RORalpha and RORgamma. *ACS chemical biology* **5:** 1029-1034

Wu J, Bostrom P, Sparks LM, Ye L, Choi JH, Giang AH, Khandekar M, Virtanen KA, Nuutila P, Schaart G, Huang K, Tu H, van Marken Lichtenbelt WD, Hoeks J, Enerback S, Schrauwen P, Spiegelman BM (2012) Beige adipocytes are a distinct type of thermogenic fat cell in mouse and human. *Cell* **150:** 366-376

Wu J, Cohen P, Spiegelman BM (2013) Adaptive thermogenesis in adipocytes: is beige the new brown? *Genes Dev* **27:** 234-250

Molecular Pharmacology Fast Forward. Published on April 22, 2015 as DOI: 10.1124/mol.114.097485
This article has not been copyedited and formatted. The final version may differ from this version.

FOOTNOTES

This work was supported in part by the by the Intramural Research Program of the National Institutes of Health National Institute of Mental Health [Grant U54-MH074404]

COI statement: None of the authors have conflicts of interest with the work presented in this manuscript. P.R.G. was a cofounder of Ember Therapeutics but they have recently shutdown. Two authors (T.J.U. and D.W.W.) were but are no longer employees of Ember Therapeutics.

Molecular Pharmacology Fast Forward. Published on April 22, 2015 as DOI: 10.1124/mol.114.097485
This article has not been copyedited and formatted. The final version may differ from this version.

Figure Legends

Figure 1. SR1555 impacts adipogenic markers. A) The chemical structure of SR1555 and B) gene expression analysis in differentiated adipocytes. 3T3-L1 cells were grown to confluence, incubated with dexamethasone, insulin and isobutylmethylxanthine (IBMX) for 2 days to induce differentiation. Cells were then treated with 20μM SR1555 and insulin for 5 days after which the expression of thermogenic genes and several nuclear receptors were analyzed by qPCR. GAPDH expression was used for normalization. Values are the mean ± SEM of 3 samples per group. *= $P < 0.05$, *** = $P < 0.001$ versus DMSO, as determined using Student's unpaired *t*-test.

Figure 2. SR1555 administration mice are resistant to obesity. A) Body weight of HFD controls and SR1555-treated obese mice, B) Food intake, and C) whole body NMR. Twenty-one week old DIO mice were administered SR1555 i.p. at 5mg/kg or 10mg/kg for 20 days. Body weight and food intake were monitored daily. Percentage fat was measured just prior to the start of compound administration and again after 17 days of compound administration. Values are the mean ± SEM of 10 samples per group. *= $P < 0.05$, **= $P<0.01$, *** = $P < 0.001$ versus vehicle or before start dosing, by Student's unpaired *t*-test.

Figure 3. Metabolic parameters in DIO mice were improved by SR1555 administration. A) cholesterol (CHOL), Triglyceride (TRIG) and free fatty acids (FFA) were measured in SR1555 treated DIO mice after 20 days dosing. B) Fasting Insulin and Insulin (0.75 U/kg) tolerance test (ITT, n=10) were measured

Molecular Pharmacology Fast Forward. Published on April 22, 2015 as DOI: 10.1124/mol.114.097485
This article has not been copyedited and formatted. The final version may differ from this version.

on DIO mice and C) glucose tolerance test GTT performed 7 days following last dose of SR1555. Values are the mean ± SEM of 10 samples per group. *= $P < 0.05$, **= $P<0.01$, *** = $P < 0.001$ versus vehicle, by Student's unpaired *t*-test.

Figure 4*. In vivo* measurement of energy expenditure and motor activity A) total oxygen consumption (VO2) B) total horizontal motor activity (XTOT), C) total vertical motor activity (ZTOT), and D) ambulatory activity count (XAMB). Mice were placed into the CLAMS for 5 days after one week of SR1555 treated obese mice. Values from all animals were pooled an average for an N=5 per group. Data were analyzed based on light and dark cycles. The light cycle occurred from 7:00am~7:00pm and dark cycle occurred from 7:00pm~7:00am in the metabolic cages. Values are the mean ± SEM of 10 samples per group. *= $P < 0.05$, **= $P<0.01$ versus vehicle, by Student's unpaired *t*-test.

Figure 5. Improvement of thermogenic genes by SR1555 and UCP1 induction. A) Immunohistochemical examination of the presence of UCP1. Inguinal adipose tissues from vehicle treated DIO mice or 10mg/kg SR1555 treated DIO mice were stained brown for UCP1 immunoreactivity. B) mRNA expression of thermogenic genes in brown fat tissue of mice fed with either Vehicle treated DIO or 10mg/kg SR1555 treated DIO. C) UCP1 mRNA expression in adipogenic C3H10T1/2 cell line. C3H10T1/2 cells were induced adipogenesis with Dex, Insulin, IBMX for 2 days then maintained with insulin and each compound for 5 days.

Molecular Pharmacology Fast Forward. Published on April 22, 2015 as DOI: 10.1124/mol.114.097485
This article has not been copyedited and formatted. The final version may differ from this version.

Figure 6. Fatty acid oxidation and modulation of mitochondrial respiration. A) Functional mitochondria content in C2C12 cells was analyzed by flow cytometry using JC-1 and red/green JC-1 (the high-low mitochondrial membrane potential) MFI ratio (right, n= 3 per condition). Mitochondria content was measured by flow cytometry analysis using Mito Tracker (MT) Green staining (n=3 per condition). B) SVF cells were grown to confluence, incubated with dexamethasone, insulin, isobutylmethylxanthine, T3, and Rosiglitazone for 2 days to induce adipocyte differentiation, and then cultured with 20μM SR1555 , insulin and T3. Oxygen consumption rates (OCR) were measured by Seahorse XF-96 flux analyzer (n= 10, 3 different condition). Values are the mean ± SEM of 10 samples per group. *= $P < 0.05$ versus DMSO, by Student's unpaired *t*-test.

Figure 1

A

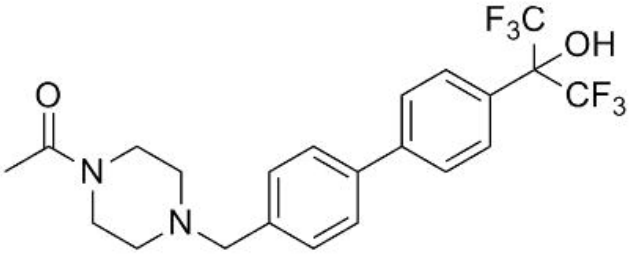
F3C
OH
CF3
O
N
N

B

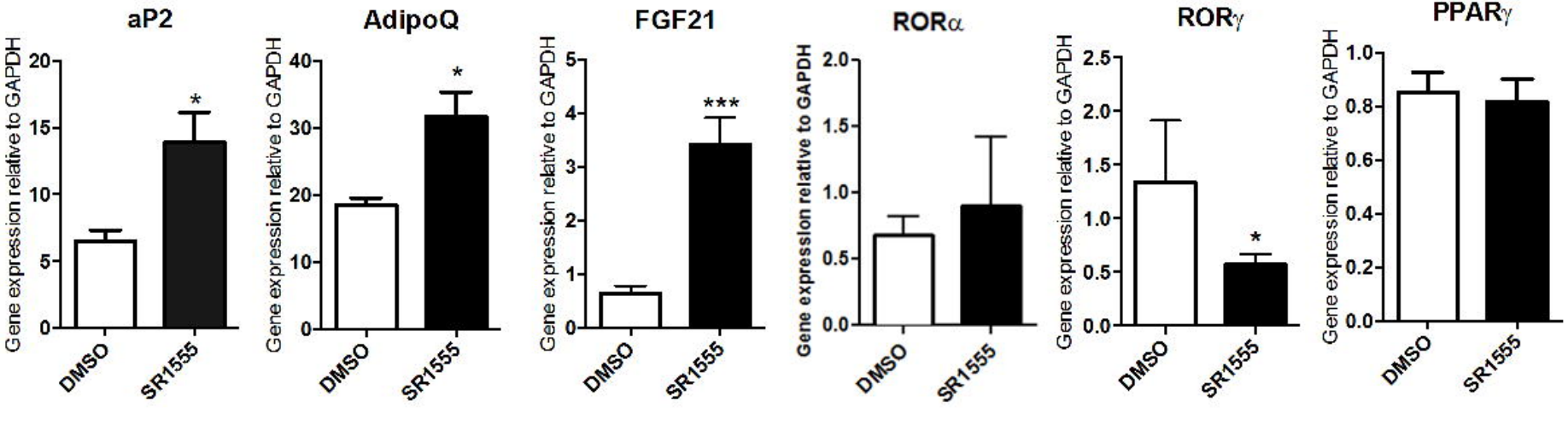
aP2
AdipoQ
FGF21
RORα
RORγ
PPARγ
Gene expression relative to GAPDH
DMSO
SR1555
*
***

Figure 2

A

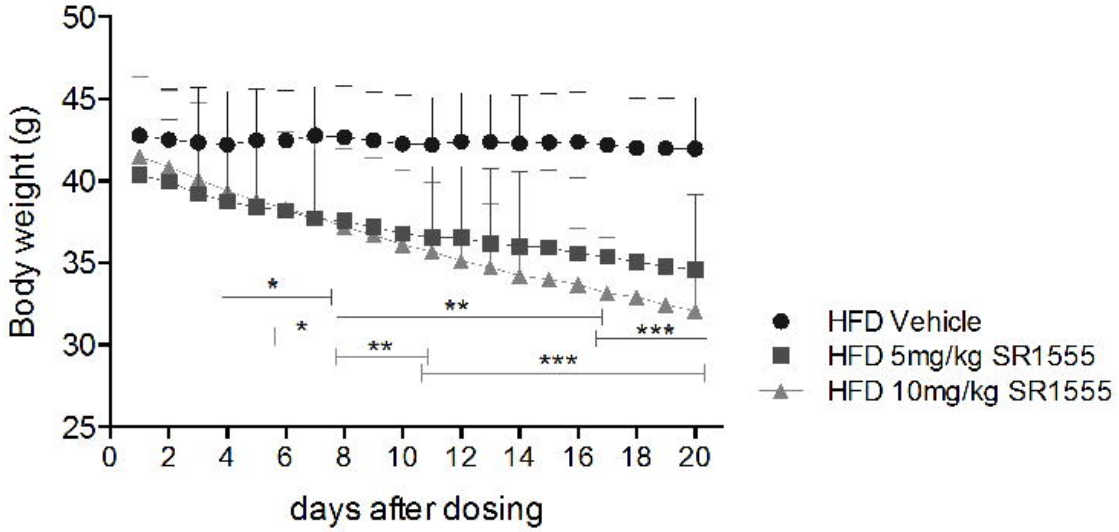
Body weight (g)
50
45
40
35
30
25
0
2
4
6
8
10
12
14
16
18
20
days after dosing
*
*
**
**
***
***
HFD Vehicle
HFD 5mg/kg SR1555
HFD 10mg/kg SR1555

B

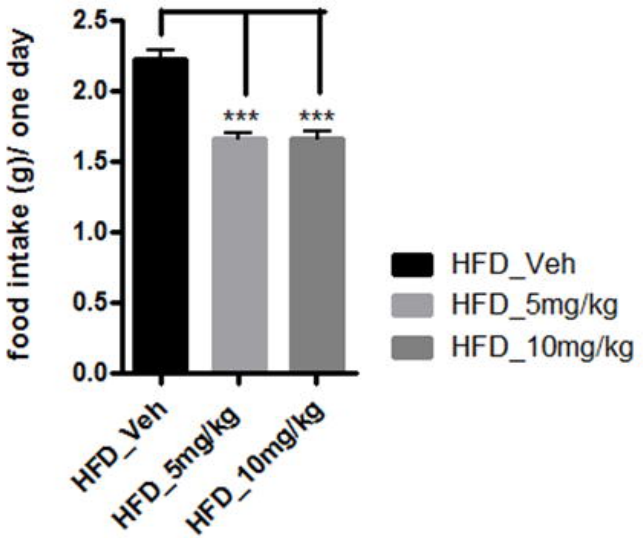
food intake (g)/ one day
2.5
2.0
1.5
1.0
0.5
0.0
***
***
HFD_Veh
HFD_5mg/kg
HFD_10mg/kg
HFD_Veh
HFD_5mg/kg
HFD_10mg/kg

C

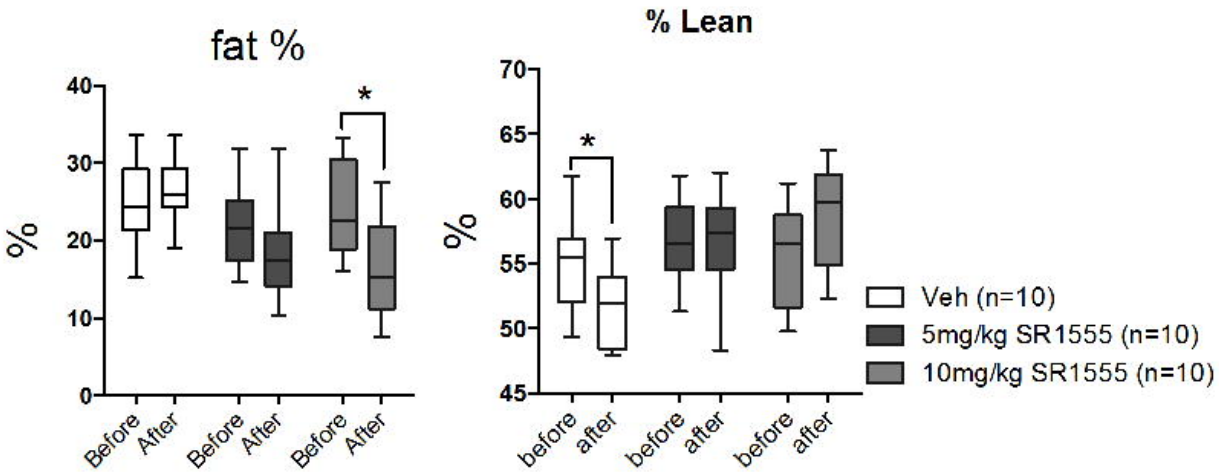
fat %
%
40
30
20
10
0
*
Before
After
Before
After
Before
After
% Lean
%
70
65
60
55
50
45
*
before
after
before
after
before
after
Veh (n=10)
5mg/kg SR1555 (n=10)
10mg/kg SR1555 (n=10)

Figure 3

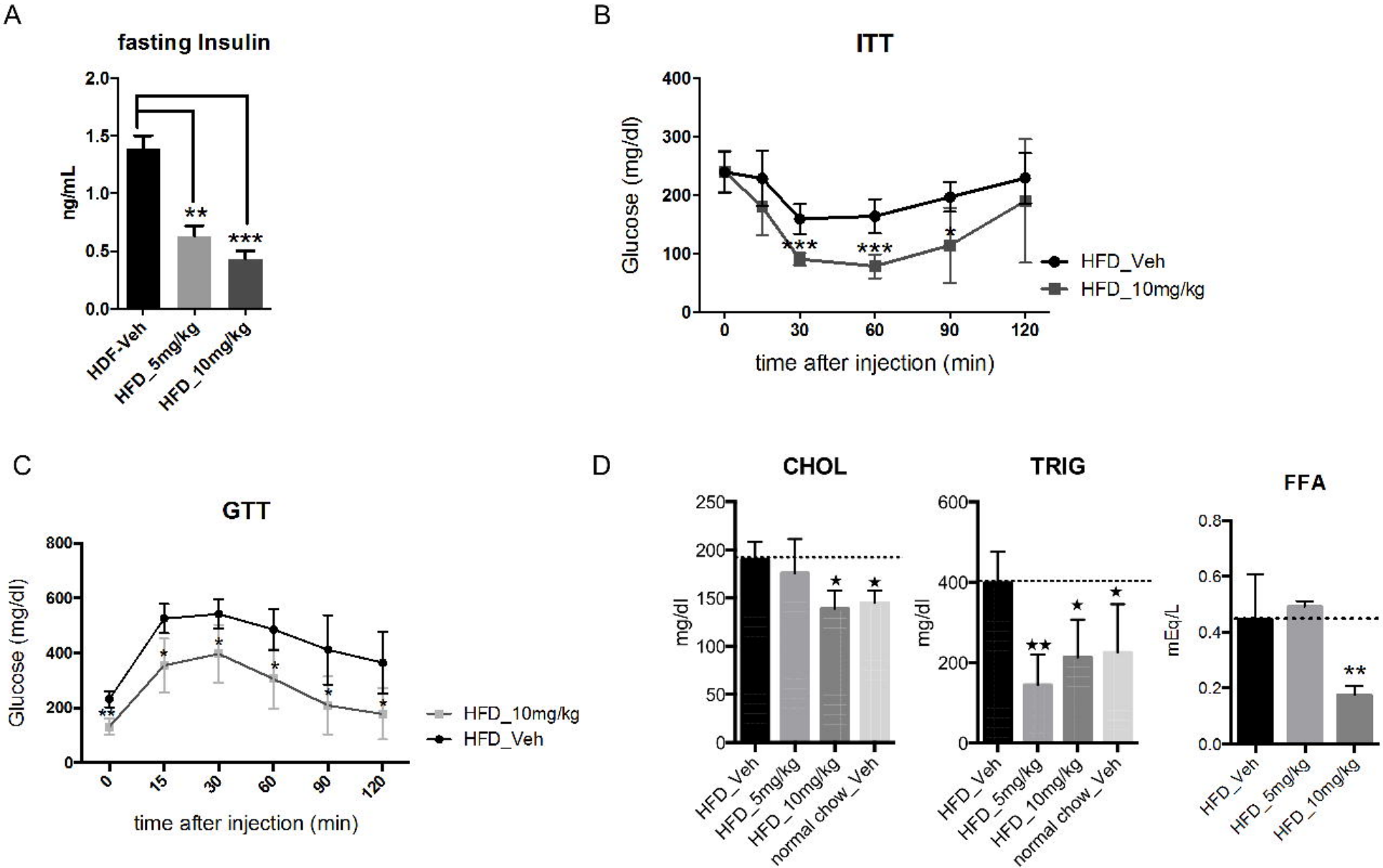
A
fasting Insulin
ng/mL
2.0
1.5
1.0
0.5
0.0
**
***
HDF-Veh
HFD_5mg/kg
HFD_10mg/kg
B
ITT
Glucose (mg/dl)
400
300
200
100
0
***
***
*
0
30
60
90
120
time after injection (min)
HFD_Veh
HFD_10mg/kg
C
GTT
Glucose (mg/dl)
800
600
400
200
0
**
*
*
*
*
*
*
0
15
30
60
90
120
time after injection (min)
HFD_10mg/kg
HFD_Veh
D
CHOL
mg/dl
250
200
150
100
50
0
HFD_Veh
HFD_5mg/kg
HFD_10mg/kg
normal chow_Veh
TRIG
mg/dl
600
400
200
0
**
HFD_Veh
HFD_5mg/kg
HFD_10mg/kg
normal chow_Veh
FFA
mEq/L
0.8
0.6
0.4
0.2
0.0
**
HFD_Veh
HFD_5mg/kg
HFD_10mg/kg

Figure 4

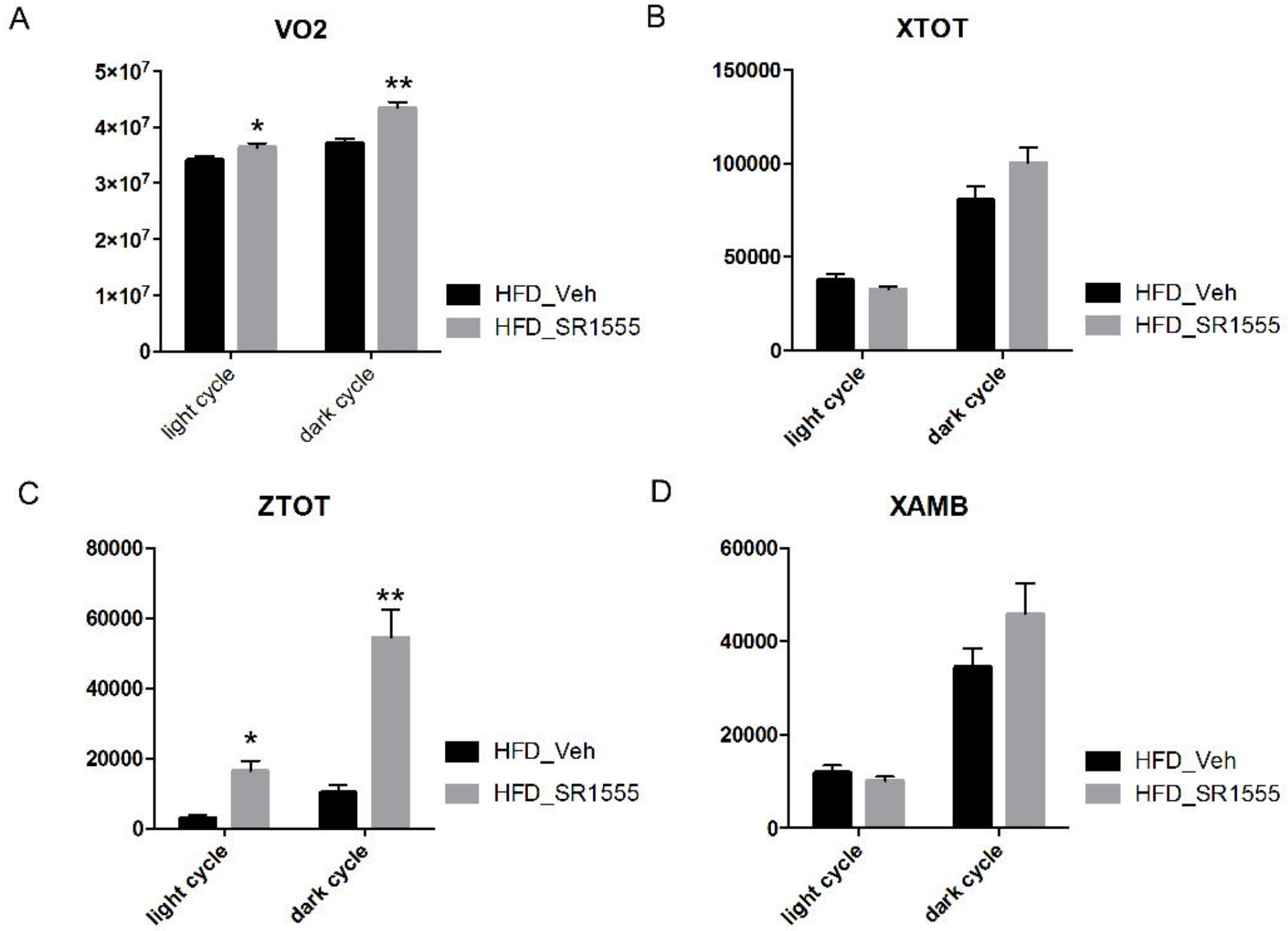
A
VO2
5×10^7
4×10^7
3×10^7
2×10^7
1×10^7
0
*
**
light cycle
dark cycle
HFD_Veh
HFD_SR1555
B
XTOT
150000
100000
50000
0
light cycle
dark cycle
HFD_Veh
HFD_SR1555
C
ZTOT
80000
60000
40000
20000
0
*
**
light cycle
dark cycle
HFD_Veh
HFD_SR1555
D
XAMB
60000
40000
20000
0
light cycle
dark cycle
HFD_Veh
HFD_SR1555

Figure 5

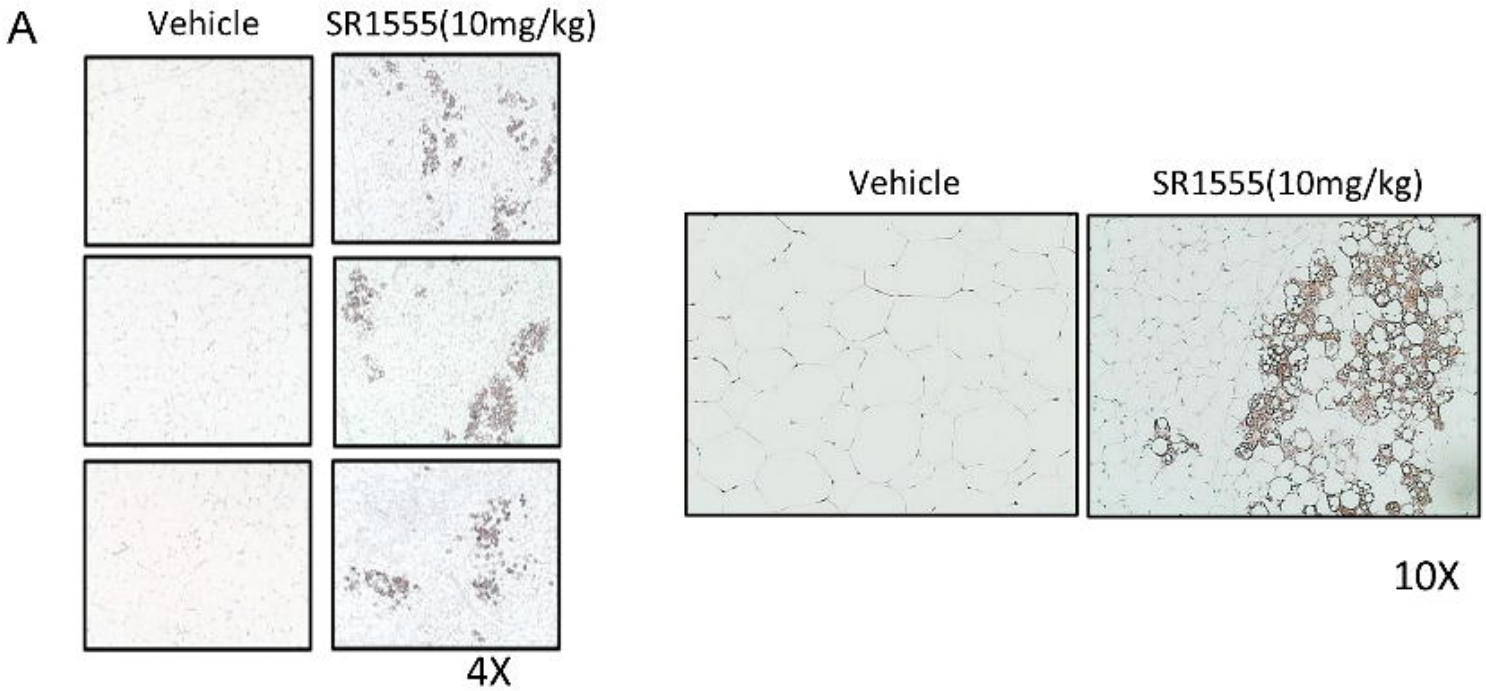
A
Vehicle
SR1555(10mg/kg)
4X
Vehicle
SR1555(10mg/kg)
10X

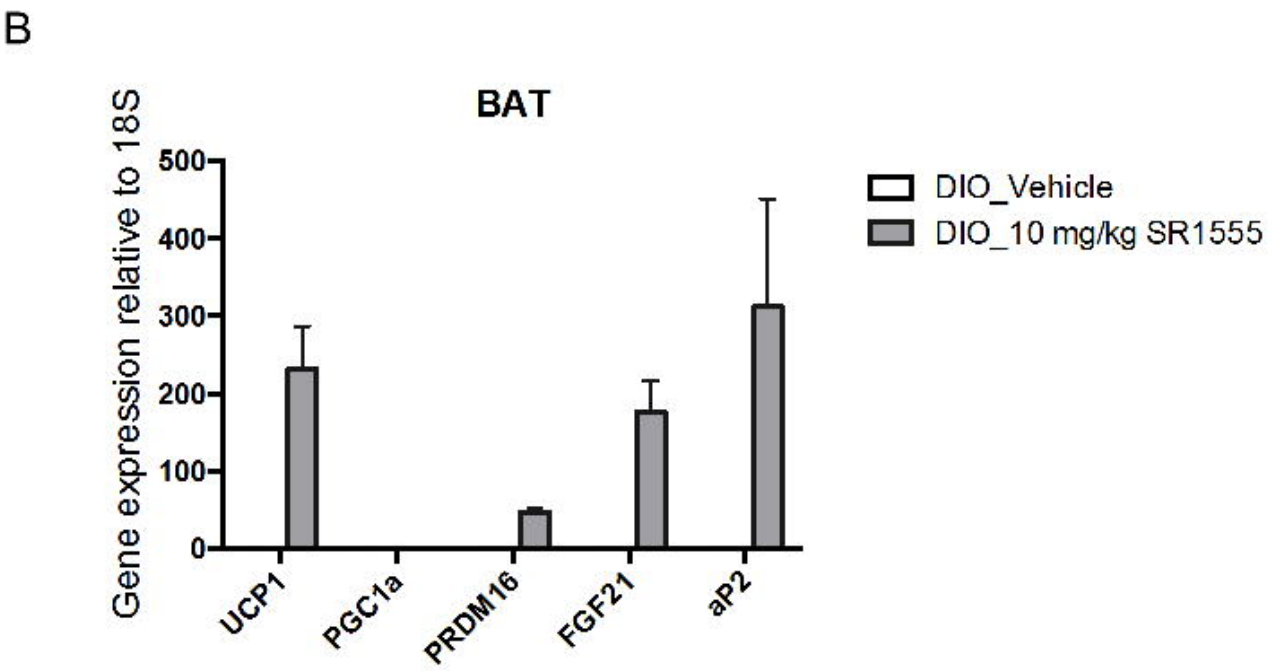
B
BAT
Gene expression relative to 18S
500
400
300
200
100
0
UCP1
PGC1a
PRDM16
FGF21
aP2
DIO_Vehicle
DIO_10 mg/kg SR1555

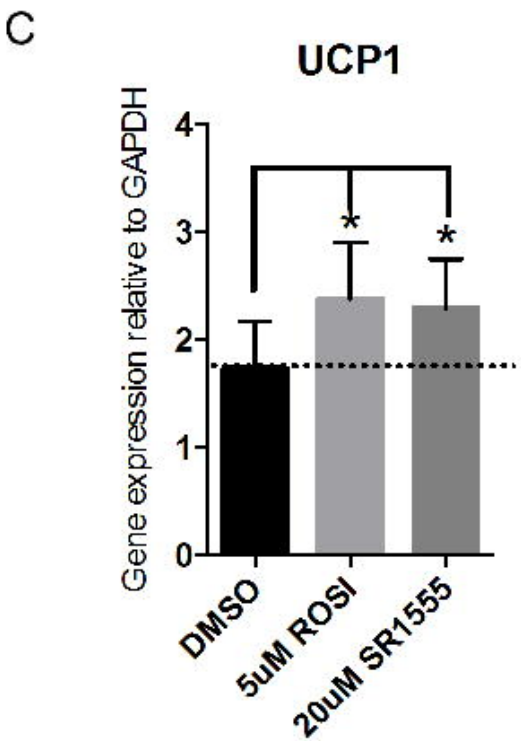
C
UCP1
Gene expression relative to GAPDH
4
3
2
1
0
*
*
DMSO
5uM ROSI
20uM SR1555

Figure 6

A

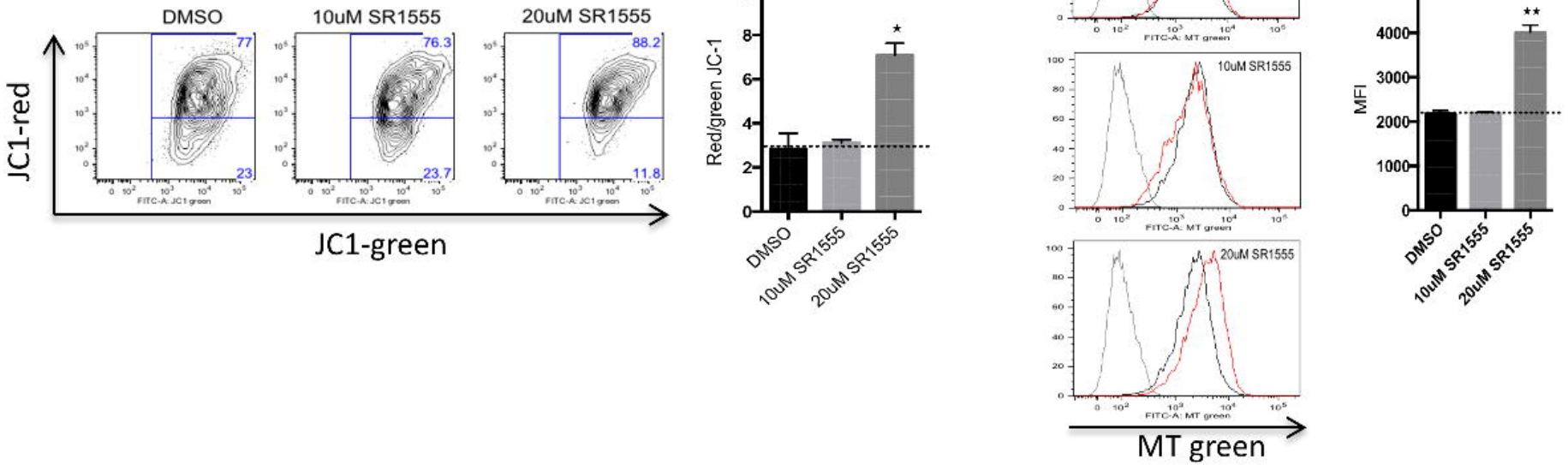
DMSO
10uM SR1555
20uM SR1555
77
23
76.3
23.7
88.2
11.8
JC1-red
JC1-green
C2C12
Red/green JC-1
DMSO
10uM SR1555
20uM SR1555
MT green
C2C12 MTgreen
MFI

B

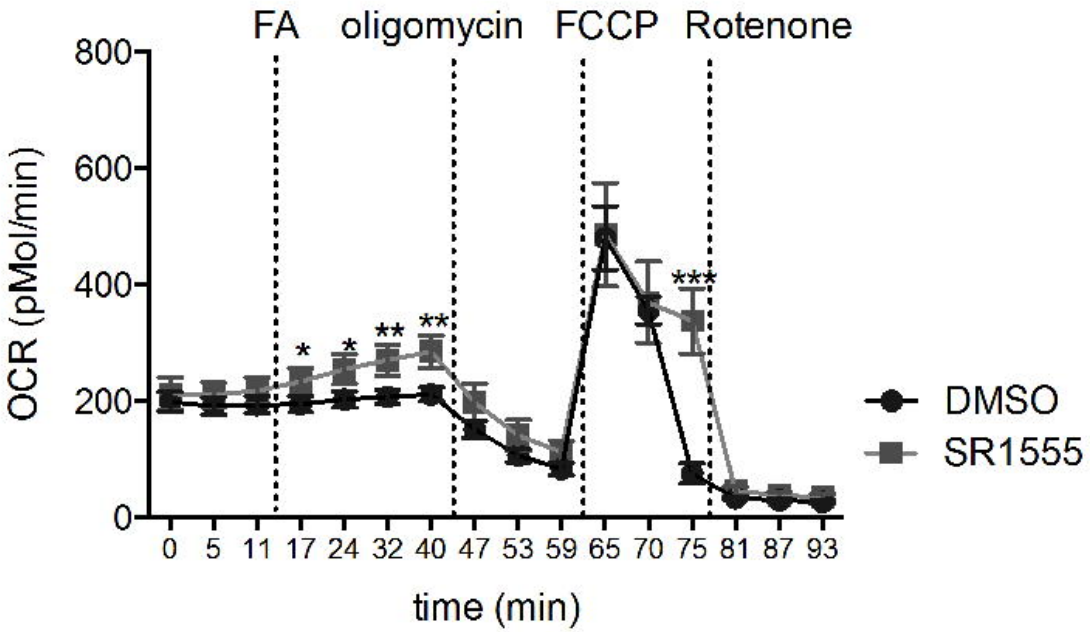
FA
oligomycin
FCCP
Rotenone
OCR (pMol/min)
time (min)
DMSO
SR1555

Supplemental Data

Molecular Pharmacology

Anti-obesity effect of a small molecule repressor of RORγ

Mi Ra Chang, Yuanjun He, Tanya Khan, Dana S. Kuruvilla, Ruben Garcia-Ordonez, Cesar Corzo, Thaddeus J Unger, David W. White, Susan Khan, Li Lin, Michael D. Cameron, Theodore M. Kamenecka, and Patrick R. Griffin

Gene name (*Mus musculus*)	Forward (5'to 3')	Reverse (5'to 3')
aP2 (FABP4)	AAG GTG AAG AGC ATC ATA ACC CT	TCA CGC CTT TCA TAA CAC ATT CC
AdipoQ	TGT TCC TCT TAA TCC TGC CCA	CCA ACC TGC ACA AGT TCC CTT
FGF21	AGC TCT CTA TGG ATC GCC TCA CTT	ACA CAT TGT AAC CGT CCT CCA GCA
RORα	CCA GCT TCC AGT CAG TGG TTA	TGC TCT GGG TCT CGA TGG T
RORγ	CCC GCC ACT CTA TAA GGA ACT CT	AGG GCT GAA GGA AAT AGA AAG TTG T
PPARγ	ACA AGA CTA CCC TTT ACT GAA ATT ACC AT	TGC GAG TGG TCT TCC ATC AC
UCP1	ACT GCC ACA CCT CCA GTC ATT	CTT TGC CTC ACT CAG GAT TGG
PGC1α	CCC TGC CAT TGT TAA GAC C	TGC TGC TGT TCC TGT TTT C
PRDM16	CAG CAC GGT GAA GCC ATT C	GCG TGC ATC CGC TTG TG

Supplemental Figure 1. Primer sequence for Q-PCR analysis

A.

B.

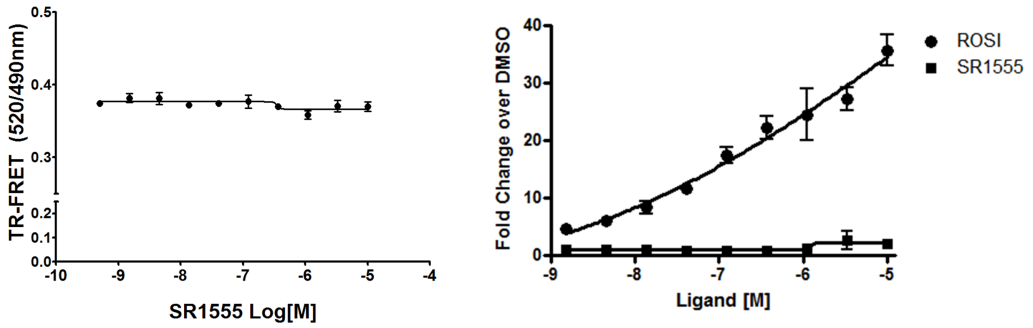

Supplemental Figure 2. PPARG activity (A) LanthaScreen PPARG TR-FRET competitive binding (B)293T cells were cotransfected with Gal4 PPARG along with UAS-luciferase plasmid. The cells were treated for 20hr with indicated concentration of SR1555 or positive control rosiglitazone (ROSI). Relative fold change was determined by normalizing to cells treated with DMSO only (no compound). Each data point was performed in 6 replicates and represented as mean ± SEM, n=6.

Time (hr)	5mg/kg IP [plasma] µM	10mg/kg IP [plasma] µM	20mg/kg PO [plasma] µM
0.25	4.0± 0.1	5.3 ± 0.2	4.4 ± 0.1
0.5	6.3 ± 0.5	8.9 ± 0.7	8.6 ± 0.7
1	6.8 ± 0.6	11.5 ± 0.4	13.6 ± 1.7
2	5.7 ± 0.1	11.6 ± 0.1	16.3 ± 0.1
4	4.1 ± 0.4	8.9 ± 1.0	16.6 ± 2.8
6	2.7 ± 0.6	5.9 ± 3.4	12.4 ± 1.7
8	1.8 ± 0.3	4.3 ± 0.4	9.8 ± 1.7
24	0.1 ± 0.0	0.3 ± 0.1	0.7 ± 0.3

Supplemental Figure 3: *In vivo* plasma drug exposure of SR1555 from bolus administration of compound at 5mg/kg IP, 10mg/kg IP, and 20mg/kg via oral gavage. N=3

Dose	$T_{1/2}$ hr	T_{max} hr	C_{max} µM	AUC_{last} µM*hr	Cl_{obs} ml/min/kg
20mg/kg PO	4.3	3.3	17.0	191	3.8

Supplemental Figure 4: Calculated PK parameters. Plasma concentrations after oral gavage dosing of 20 mg/kg SR1555 were determined and fit to a noncompartimental model in WinNonlin.

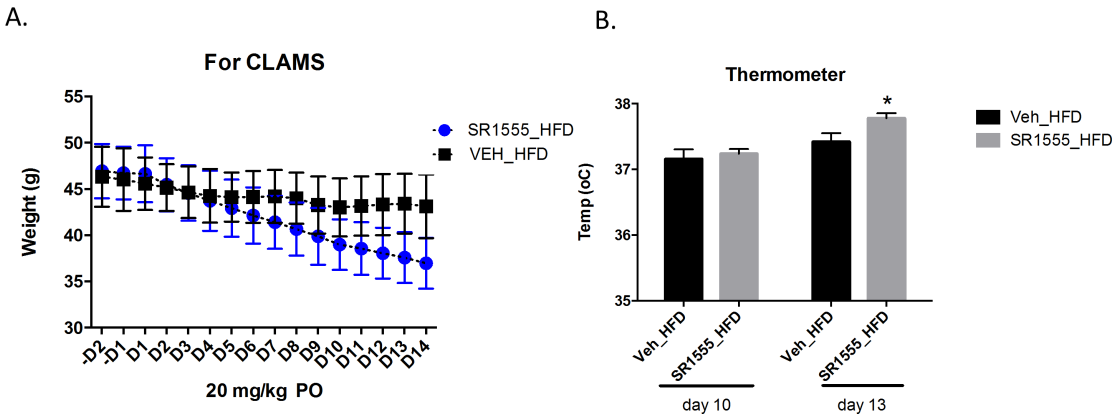

Supplemental Figure 5: DIO mice were administered SR1555 20mg/kg orally 14 days. A) Body weight and B) body temperature at days 10 and 13. Body temperature was recorded with a rectal probe connected to digital thermometer (BA T-12 Microprobe-Thermometer, Physitemp, Clifton, New Jersey, USA).

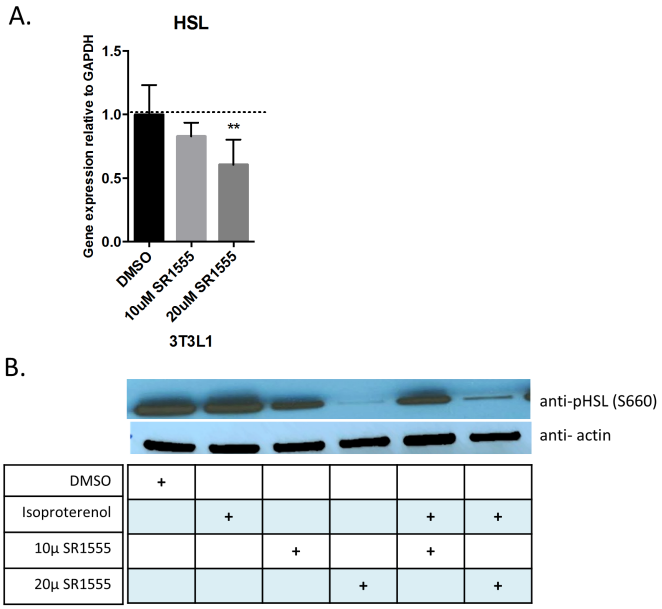

Supplement Figure 6. HSL activity. Differentiated 3T3L1 cells were incubated with 10µM isoproterenol for 30min to stimulated lipolysis. Relative mRNA level was measured by qPCR (A) and phosphorylated HSL (Ser660) was detected by western blot and actin was used for control (B)

A.

Seq. name	Accession no.	Gene symbol	Start position	End position	Strand	Consensus Sequence
Promoter1	NC_000073	Lipe	238	244	+	ATTTGGG
Promoter1	NC_000073	Lipe	348	354	-	ATCTGGG
Promoter1	NC_000073	Lipe	431	437	-	AAATAGG
Promoter1	NC_000073	Lipe	549	555	+	AAGTGGG
Promoter2	NC_000073	Lipe	397	403	+	AACTGGG
Promoter2	NC_000073	Lipe	607	613	+	AACTAGG
Promoter2	NC_000073	Lipe	874	880	+	AAGTGGG
Promoter3	NC_000073	Lipe	456	462	-	AACTGGG

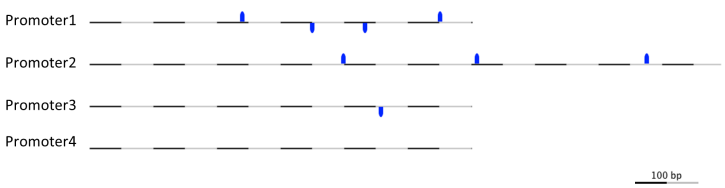

B.

- >Promoter1|sym=Lipe|taxid=10090|spec=Mus musculus|chr=7|ctg=NC_000073|str=(-)|start=26183628|end=26184229|len=602|comm=Promoter Region
AGGGTTTTGAGCCTATAAAAACAGGATGGTATGTGCTTTGTTTTGTTTTGTTTCCTTTTTAGTAGGAGTTATAAAATGAT
CAGAGCAACAGTCTAAGACAATTCAAAAGGCAACCAAGTTGTAAGAATGAATGAAAAGGAAACTATGATTAAAAGTATAA
AGACTCCTTAAGTATTCCTCTGGTATCAGGAGGGGGAAAAGTACTGAACTATAGTGGTACACACCTGTGGTCACAGAATT
TGGGAAATGAAGACAGGAAGAATAGTAGTAGCTTGAGGCCAGCCTGGGCTACATGAGTTTCCCATCTCTGGGGGTAGGGA
CCACTCATCTAGCTCACCTAGAATCATCCCAGATGAAACAGAAGACTAAGATACTTGCCTTATGAGAAGGGTCACTGGTC
ATTTTAACTGAGTGGTGAGTGGGGCGGGGCCCTATTTATGACACAAGAGAACAAGCCCCTCCCTTCTTGTAAGACAGTAC
TGGGCACATGAGCCTCTTCCTAGTCCTAATCCCTCTCCCAAAGAGACACAGAGAGATCACCTGGCAAGAAGTGGGGACCA
GCAGTGATAAACTCACAGATCAGCTATAAAGGAAGATCAGGA

- >Promoter2|sym=Lipe|taxid=10090|spec=Mus musculus|chr=7|ctg=NC_000073|str=(-)|start=26180906|end=26181898|len=993|comm=Promoter Region
CTCAGCGCCGTGGAATGACTAGATTTCATGGGGTAGAGAAGCTTGGGAGCAGGGCCTGGATAGGGCTGCAGAGGTCTGTG
GCAAGATCCAGGCGGAATGGAAACAGCGTAGTGAAGTGCTGGTGAGCTGTGGCGCTTCTTCCTTGCCGCCTCTCCGAAGC
AATGGCAGGTAACAGCCATAGGACCCAGTCCTGACAGGAGCAGAGGGAAGGTCAGAGTCCTGAGGGCCGCTAGTGATGGT
CTTTCACCTCAGAGGGCCGTCCCTCCTCCCCAAAAGCCTGAGAGGTTTCTCCGAGGACAGAGTAATTAATGCTCACTCTG
TCAAGAAGAAAATCGAGGCTTAATCCTCCCAGGGCAGCCGGGTTCCAGAAGCTTCTGGCATGGGCAACCCAGAAGCAACT
GGGAGCACAGTGAGCCATGTGCGCATGTGCGAGTCTCGGGCCTCCTCTGTTTCCCGCCTTTTCCGGGGCACGTGGGCTCC
CTCGACTTACGCTCCTTTCTGTAGATCAACCCTGAGGCCGGCGGTGTTGCTGTCTTCCCCTTTCCTTTGATTCTGGGGAA
TAAGGCAGGGCAGAGGGAGAGACACCTCATGAAGCAGAGCAGTAAGAACTAGGAGGGAGCGCGGATGTGAGACTGGAAGG
TAGTTTGCTGAGAGGCCAAGGCCACCCTCAACTACAGCCTAGGACCCTGTCTGGGGGGGAAAAAAAAAAAAAAAAAAAAA
AAAAAAACAGGGACGACCACGTGAGGGGGCGGAGGAAAAGGCGGGGCTTCTCCAAACGGCTACCAAGCGCGGCTACGCCC
CCAAGTCGGTCCCCGCCCACGCCTTGGGTTGCCCGCCCCCTGCCCGCCCGCCCGTTCTTCCGGCTCCCGGGGCAAGTGGG
CGGGCCAGGTTCAAGGAAAGGTGAATGAGATGGCGAGGGTCAGCACCTGCACAAGATGACTGAGAATTCTTTGTTGGGGT
GACTCTAACGCGACTCCTCACTATTCCTGCTGT

- >Promoter3|sym=Lipe|taxid=10090|spec=Mus musculus|chr=7|ctg=NC_000073|str=(-)|start=26175025|end=26175625|len=601|comm=Promoter Region
ACAGCAGGGCTGGCCACTTCTTTTCCCTAACAGCTGGAGACATCTGTGCCAGGGCCAATGTCGGGAGGGGGGGGAATTGGC
ATAACTGAGCCTTTGGCTCCCTGAATCCACTTGGGGGAGAGGAGAGGACAGCTTTCTGGGGGAGAGGGGACAGTGTGTTC
AGGACTAAAGCTTGGGACTCCTGGGTCCTAAGGGAGAAGACTGGAACTGGATCCCCGAGTCTGAGCAAGGAGAGCCTGGG
CCTGGGCTCCCTGGTGTAAGCAAGGAGGGGCTGAGAGGGCAGGGATCCAGGGCTCTGAGGAAGAACCTAGCAGGAGGACT
CTGTTGAGCTGCCTGTCCAGCAGGCAGGAGGGGCAAGGAGTTGAACTCTGGGCTCTGTTTACAGCATGTGGTTCTCACTA
TCCTTTCTGGATAGGAGGTGAAGCAGTGGCCACACCCTACCCCACTAGTCCCTCCCCCAGTTTATCGCCCCAGGCTGCTA
CTGGCACTAGCCACAGACCTGCTGTGCCAGCTTGGGGAGCTCCAGTCGGAAGAGGCCAGGGAGGGGTGAGTGCAGGCCCA
ACCAAGAGACAGAACCCAGGGCCTGGAGGGGAGAGGAGACA

- >Promoter4|sym=Lipe|taxid=10090|spec=Mus musculus|chr=7|ctg=NC_000073|str=(-)|start=26165828|end=26166428|len=601|comm=Promoter Region
CAGTAGAGCGCCTGCCTGGAATCCACCAGTGAGGGAGGGAGGGGCAAGAGCCTAGGAACTAGCCTGTGCAAGGACTATGT
GCACCACAGAGACAAAAATTAATACAGATGCATCTTGATTCCTCTGGAGGAAAGGTTGGTAATCCTGGGTTCTTGTATTC
TTGTAACTTAAAAGCTAAGTACTATAAAACATTTATACAGAGGGAAAAAATGGAAGCTTTCAGAAGTCAGTTGATTTGCA
CTTCCCAGTCTTAATACATGCACACCCTCCACTATAACACAGCCCCACCTCCAAGACTACCAGCCTTAGGATTGCAACCC
TGGATACAGAAATGTCCCATTCTGGAGGGGGTGGTTGGTCCCGGACTGCCCCCTGTCTGGCATCCACACACCCTACTCAC
GGCCAGGCTTATCTTCTGGCCTCAGGCAGCCTCTGTCTTTGCTTTTCCTATAGAGTCTGTGCGCCCCACGGAGTCTATGC
GCAGGAGTGTGTCTGAGGCAGCCCTGGCCCAGCCTGAGGGCTTACTGGGCACAGATACCTTGAAGAAGCTGACAATAAAG
GACTTGAGCAACTCAGAGCCTTCAGACAGCCCCGAGATGTC

Supplemental Figure 7. (A) ROR response elements in the promoter of HSL (B) HSL promoter sequence contained RORE